Heat Transfer and Fluid Flow Analysis of A Fluidized Bed Reactor for Beam-Down Optics

Selvan Bellan[1, 3 a)], Tatsuya Kodama [2, 3, b)] Koji Matsubara[2,3], Nobuyuki Gokon[1,3] and Hyun Seok Cho[3,4]

[1]*Center for Transdisciplinary Research, Niigata University, 8050 Ikarashi 2-nocho, Niigata 950-2181, Japan.*
[2]*Faculty of Engineering, Niigata University, 8050 Ikarashi 2-nocho, Niigata 950-2181, Japan.*
[3]*Pacific Rim Solar Fuels Research Center, Niigata University, 8050 Ikarashi 2-nocho, Niigata 950-2181, Japan.*
[4]*Institute of Science and Technology, Niigata University, 8050 Ikarashi 2-nocho, Niigata 950-2181, Japan.*
[a)]*Corresponding author: selvan@niigata-u.ac.jp*
[b)] *tkodama@eng.niigata-u.ac.jp*

Abstract. A transient three dimensional numerical model of the heat transfer and fluid flow of a windowed fluidized bed reactor for solar thermochemical conversions is formulated and solved using discrete element method coupled to computational fluid dynamics. Radiation transfer equation is solved by discrete ordinate radiation model and the particle collision dynamics is solved by spring-dashpot model based on soft-sphere method. The instantaneous granular flow behavior of the irradiated bed is presented along with the incident radiation and particle size distribution. The results indicate that as time progresses the average velocity of the particle increases due to high temperature and bed expansion effect.

INTRODUCTION

The two-step water splitting of redox materials is one of the promising processes for converting concentrated solar high-temperature heat into syngas in sun-belt regions [1-2]. Nakamura [3] initially proposed a two-step water-splitting cycle by a redox pair of Fe_3O_4/FeO, and conducted a thermodynamic analysis. As this redox pair required high reduction temperature, mixed solution of Fe_3O_4/FeO and M_3O_4/MO was tested to reduce the reduction temperature [4]. In recent years, non-stoichiometric cerium oxides have emerged as highly attractive redox materials due to its high melting temperature, fast oxygen-ion transport and high oxidation rates. Recently, various fluidized bed reactors have been developed and tested at Niigata University, Japan, for two-step thermochemical water splitting cycles and coal coke gasification using Xe light solar simulator [2]. The hydrodynamic behavior of the gas-solid flow plays a vital role on the performance of the fluidized bed reactors. The flow characteristics of the bed can be obtained by some experimental techniques such as particle image velocimetry, digital image analysis, and etc. However, it is pretty challenging to use these equipments in our experiments due to high temperature and radiation fluxes. Numerical modeling is one of the appropriate methods to obtain a fair insight of heat transfer and fluid flow of the gas-solid flow behavior [5-7]. Thus, various Lagrangian-Eulerian and Eulerian-Eulerian numerical models were developed to study the fluidized bed flows. In Lagrangian-Eulerian method, the fluid phase is treated as continuum and solved using computational fluid dynamics (CFD) approach while the particles are tracked individually in space and time by using discrete element method (DEM).

Although several CFD-DEM studies were performed on fluidized bed rectors, only a few studies were conducted at high temperature ranges (> 600 K) for solar thermal applications [6-10]. A laboratory scale solar particle receiver was developed at the National Renewable Energy Laboratory for use in concentrating solar power plants [8]. The prototype consisting of enclosed arrays of hexagonal heat transfer tubes. Simulations were performed for different geometric configurations, hexagon apex angles, particle sizes and mass flow rates, and reported that the heat transfer strongly depends on the particle size and at higher solid mass flow rates, more particles contact the heat transfer

surfaces and the overall heat transfer increases. Early designs of particle heating receivers (PHR) utilize a falling curtain of particles which directly absorbs the concentrated solar radiation. Since the falling curtain receivers have several disadvantages including significant heat and particle losses and short residence time within the irradiation zone, the so called "impeded flow PHR design" was proposed to overcomes these challenges, in which the particles flow through a series of obstacles in the flow path. Hence, it reduces heat loss, particle loss and average velocity of the particles, thereby increasing their residence time in the irradiation zone of the receiver. Since the particulate flows through complex structures are not well understood, a numerical model was developed by Sandlin et al.[9] to better understand these flows. Recently, we have developed a model to investigate the granular flow and heat transfer characteristics of a two-tower fluidized bed reactor, which consisted of two rectangular chambers placed side by side and connected by two interaction ports [10]. The large tower in the left hand side was irradiated by solar radiation and the heated particles were moved to the small tower through top interaction port by drag force of gas stream. This reactor can be simultaneously used as particle receiver (large tower) and storage system (small tower). Then, flow and heat transfer analysis of 5kW_{th} spouted fluidized bed reactor, consisting of two separate inlets (spout and annulus) to create circulating fluidized bed, was studied [6-7]. The influence of spout and annulus gas flow rate [6] and particle size [7] on the solid-gas flow and heat transfer characteristics of the reactor was studied. In this study, the granular flow and heat transfer characteristics of the 30 kW_{th} prototype fluidized bed reactor has been investigated and the interaction of concentrated radiation with the fluidized bed has been presented as a function of time.

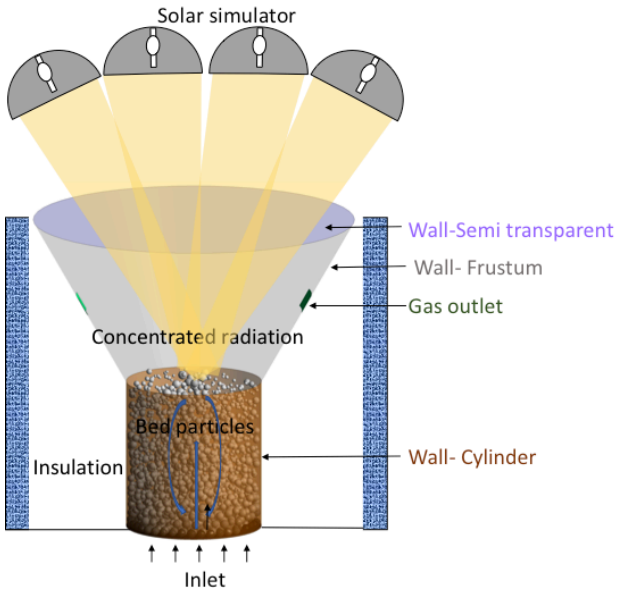

FIGURE 1. Schematic and computational geometry of the reactor

NUMERICAL MODEL

The fluid flow of the gas-phase is simulated from the volume-averaged Navier–Stokes equations whereas the motion of every individual particle is tracked by Newton's second law. To predict the thermo-fluid flow, the conservation of mass, momentum and energy equations of the gas phase are formulated as follows;

$$\frac{\partial}{\partial t}\left(\alpha_f \rho_f\right) + \nabla.\left(\alpha_f \rho_f \vec{u}_f\right) = 0 \tag{1}$$

$$\frac{\partial}{\partial t}\left(\alpha_f \rho_f \vec{u}_f\right) + \nabla.\left(\alpha_f \rho_f \vec{u}_f \vec{u}_f\right) = -\alpha_f \nabla p + \nabla.\left(\alpha_f \bar{\bar{\tau}}_f\right) + \alpha_f \rho_f \vec{g} + \vec{F}_{DEM} \tag{2}$$

$$\frac{\partial}{\partial t}\left(\alpha_f \rho_f C_{p,f} T_f\right) + \nabla.\left(\alpha_f \rho_f \vec{u}_f C_{p,f} T_f\right) = \nabla.\left(\alpha_f k_{f,eff} \nabla T_f\right) + Q_p + Q_{rad} \tag{3}$$

where ρ_f , α_f, $\vec{u}_f$, g, p, $\bar{\bar{\tau}}_f$, $k_{f,eff}$, $C_{p,f}$ and T_f are density, volume fraction, velocity, acceleration due to gravity, pressure, stress–strain tensor, effective thermal conductivity, specific heat and temperature of the gas phase respectively. In this model, the moving particles are considered as moving mass points and the fluid flow details around the particles, such as boundary layers, vortex shedding, are neglected. Discrete ordinates (DO) radiation model has been used to solve the following radiative transfer equation. A detailed description of the governing equations and particle-particle interactions can be found in e.g. [6, 10-11].

The Schematic and computational geometry of the reactor is shown in **FIGURE 1**. The reactor consisted of a cylindrical (0.16 m diameter and 0.175 m height) and a frustum shape (0.195 m height) chambers. The reactor was closed by 0.38 m diameter quarts window on the top of the frustum chamber. The outer part of the cylindrical reaction chamber contained an annular electric heater to pre-heat the bed. In order to avoid heat losses, the reactor was insulated and then covered by a stainless steel outer chamber. The temperature dependent thermo-physical properties of the N_2 gas were obtained from ref. [6] and the particle properties are given in **TABLE 1**. The spring stiffness, restitution coefficient and friction coefficient were obtained from the experimental results and literature [12]. Boundary conditions are given in **TABLE 2**.

TABLE 1. Thermo-physical properties and modeling parameters of particles

Properties	**Geldart D**
Density [kg/m^3]	2600
Specific heat [J/kg-K]	$-3x10^{-05}T^2 + 0.0696T + 633.46$
Thermal conductivity [W/m-K]	$-1 \times 10^{-09}T^3 + 3 \times 10^{-06} T^2 - 0.0007 T + 1.3834$
Diameter [μm]	200-300
Shape	spherical
Coefficient of restitution	0.9
Coefficient of friction	0.3

In **TABLE 2**, σ, ε, n are Stefan-Boltzmann constant, emissivity and refractive index respectively. To solve the radiative transfer equation, walls and particles are assumed as gray and diffuse. The net radiative flux from the walls is computed as a sum of the reflected portion of incident radiation and the emissive power of the surface. At walls, the radiation intensity for all outgoing directions is q_{rad}/π. At semi-transparent wall, the irradiation beam (q_{irrad}) is applied by the magnitude, beam direction and beam width based on the experimental measurements. The external heat transfer coefficient, h_{ext}, is calculated based on the thermal resistance caused by the insulation layer [13]. The net radiative heat flux at the inlet and outlet is computed in the same manner as at walls by assuming the emissivity= 1.0 (black body absorption). The control volume technique has been used to solve the governing equations.

To validate the flow behavior of the model, recently a transparent two tower fluidized bed reactor was developed. The reactor consisted of two rectangular chambers placed side by side and connected by couple of interaction ports. Each chamber was filled with different color of powder to obtain the particulate flow pattern between the two towers. Since the superficial gas velocity of the left tower was higher than the right tower, the particles circulation pattern was occurred in clockwise direction. Simulation was performed for the same operating conditions and the predicted particulate flow pattern was comparable with experimental results [5]. Then the developed model was applied to predict the heat transfer characteristics of the fluidized bed reactor and a fair agreement was found between the experimental and numerical results [7].

RESULTS AND DISCUSSION

Since the main purpose of this investigation was to analyze the thermal performance of the bed, chemically inert particles were considered. About 3.3 kg of powder, with particle size from 100 μm to 300 μm, was filled. The size distribution was defined by the mass fraction of 0.05 for every 10 μm interval. The bed was preheated by an annular electric heater up to 973 K. Then, the bed was fluidized by N_2 gas at 25 L/min flow rate and irradiated by concentrated radiation (19 kW_{th}) using 13 xenon arc lamps. However, the irradiation power can be increased up to 30 kW_{th} using 19 Xenon arc lamps [2]. The incident concentrated radiation covers the focal plane about 0.2 m diameter. **FIGURE 2** shows the three dimensional temperature distribution of the discrete phase particle along with the incident radiation at different instants.

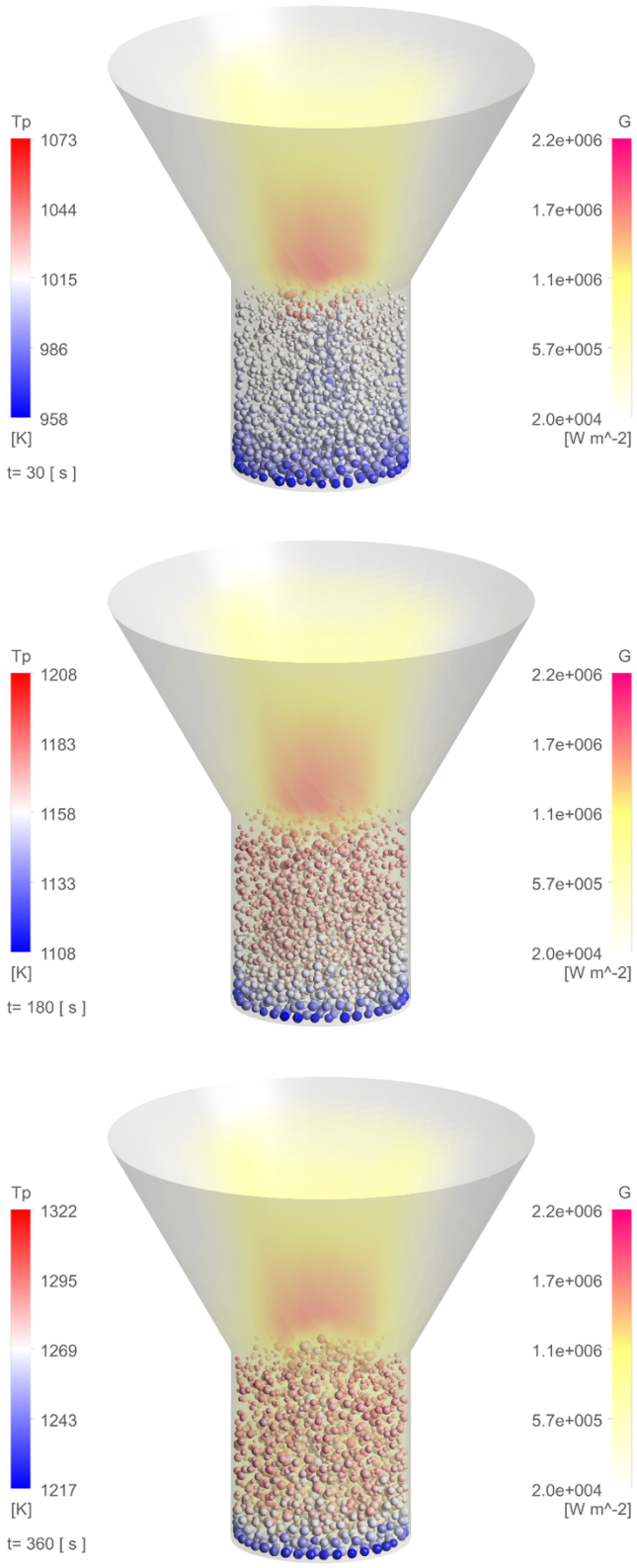

FIGURE 2. Three dimensional temperature distribution of the discrete phase particle along with the incident radiation at different instants.

In each figure, the legends in the left and right hand sides respectively represent the temperature of the discrete phase and incident radiation respectively. Since the porosity of the gas distributor at the bottom of the reaction chamber decreases along the radial direction, it creates Gaussian like velocity distribution. The higher velocity gas at the central axis region creates bubbling fluidization and drag the particles in the central axis region to the top of the bed and creates "fountain core". Then the sprayed particles move to the fountain periphery due to the relatively lower velocity and drag force and then move to the inlet through annulus. As the top surface of the fountain is continuously irradiated, as can be seen in the figure, the fountain core particles are heated up, concurrently the incident radiation is scattered by the fountain region particles. The scatted radiation is diffused throughout the bed and part of the incident radiation is reflected back. Although the top part of the bed is heated up, the carrier gas at atmospheric temperature is entered through the inlet and extracted the heat from the particles, right from the inlet to the fountain, and transferred the heat to the frustum part and left through the outlets. So, the maximum temperature difference is found between the fountain and inlet.

TABLE 2. Boundary conditions

Section	**Velocity $\vec{u}_f$**	**Temperature**	**Radiation**
Wall-Cylinder	0.0	$q = h_{ext}(T_{ext} - T_w) + \varepsilon_{ext}\sigma(T_{ext}^4 - T_w^4)$	$q_{rad} = (1-\varepsilon_w)q_{in} + n^2\varepsilon_w\sigma T_w^4$
Wall-Frustum	0.0	$q = h_{ext}(T_{ext} - T_w) + \varepsilon_{ext}\sigma(T_{ext}^4 - T_w^4)$	$q_{rad} = (1-\varepsilon_w)q_{in} + n^2\varepsilon_w\sigma T_w^4$
Wall-Semi-transparent	0.0	$q = h_{ext}(T_{ext} - T_w) + \epsilon_{ext}\sigma(T_\infty^4 - T_w^4)$	q_{irrad}
Inlet	u_f (m/s)	Temperature (K)	Black body
Outlet	$\frac{\partial \vec{u}_f}{\partial n} = 0$	$\frac{\partial T}{\partial n} = 0$	Black body

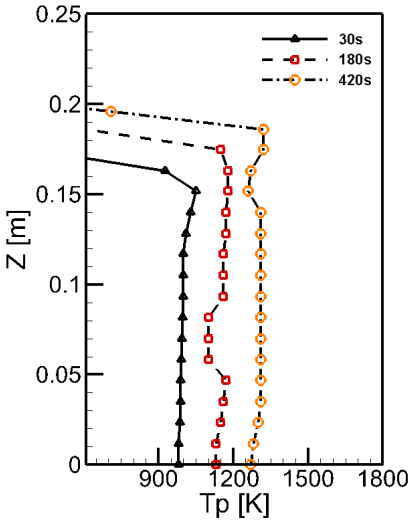

FIGURE 3. Instantaneous temperature distribution of the particle phase at the central axis.

FIGURE 3 shows the instantaneous temperature distribution of the particle phase at the central axis. As the fluidization rate is adequate, the temperature gradient of the bed is small. Despite the particles close to the inlet are cooled down by the carrier gas, the temperature of the bed is increased due to continuous irradiation with fluidization. At high temperature, the density of the gas decreases and subsequently the velocity of the gas increases and expands the bed. Hence, the higher bed porosity enhances the diffusion rate of the scattered radiation at the fountain core. Furthermore, the high temperature particles also emit significant amount of radiation. The cumulative diffused radiation can be apparently seen at t= 360 s of **FIGURE 2**.

FIGURE 4 shows the particle size distribution at different instants, at 1, 180 and 360 s. It can be noted that, initially the particle size distribution is random but after few rounds of fluidization, the large size particles are segregated close to the bottom inlet region due to gravitational force. Since the gas velocity at the inlet-central axis (drag force) is adequate to transport the segregated large size particles close to inlet, the particles are moved over the

central axis spout jet region. Thus, the top fountain and annulus parts of the bed predominantly governed by the small size particles, which could enhance the heat transfer rate due to the larger surface area to volume ratio.

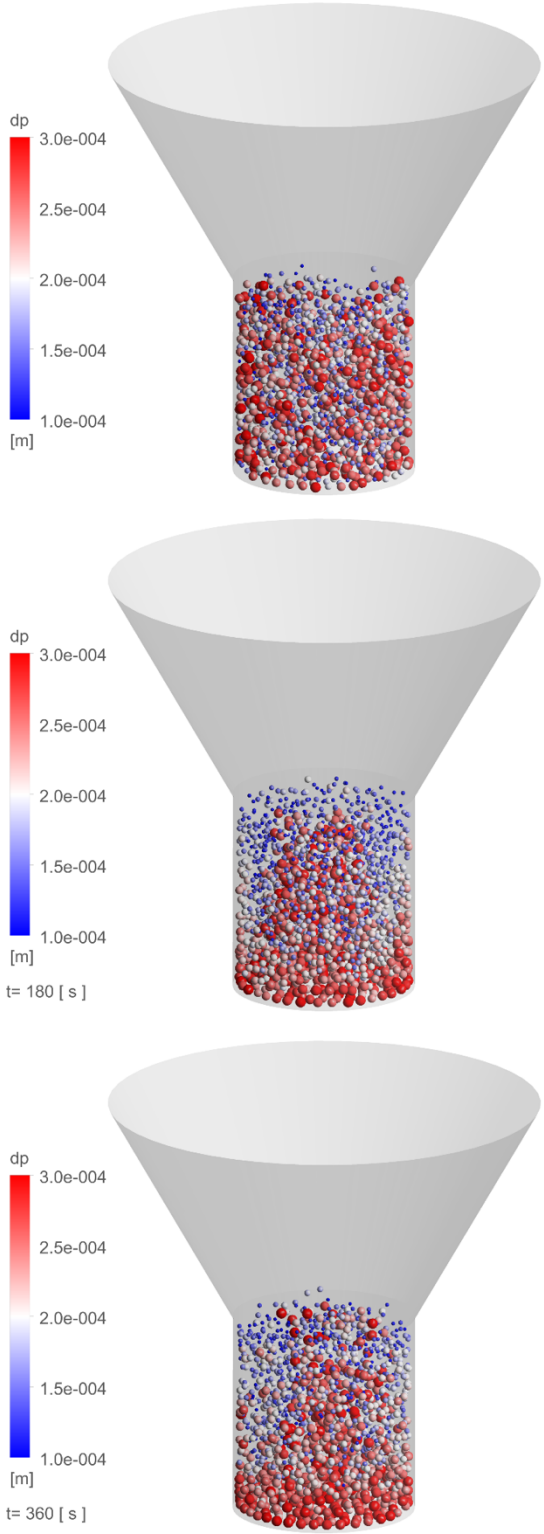

FIGURE 4. Particle size distribution at different instants, at 1, 180 and 360 s.

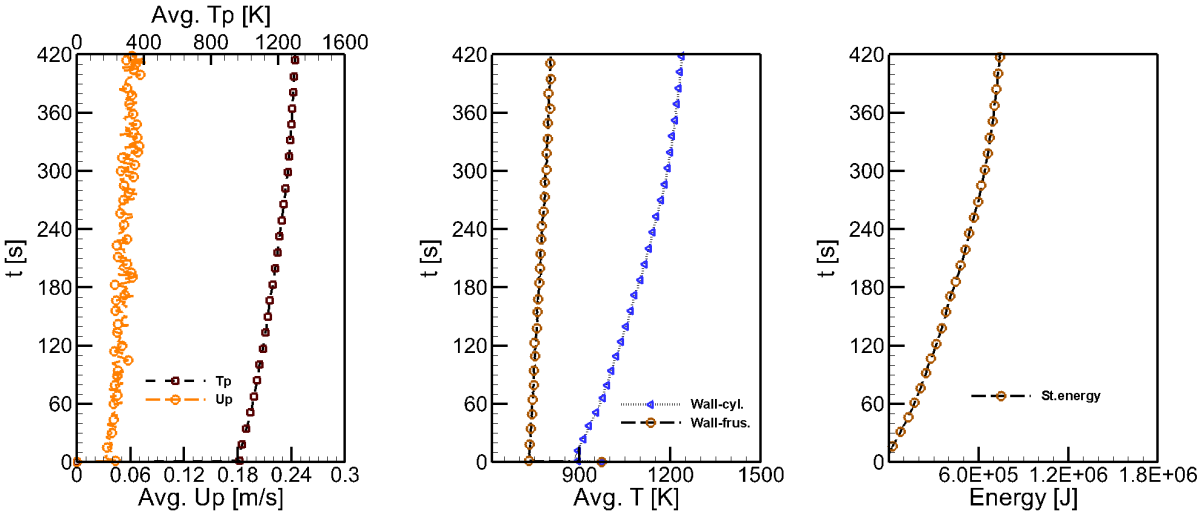

FIGURE 5. Average temperature and velocity of the particles as a function of time along with the average wall temperature and total energy stored in the bed.

FIGURE 5 shows the average temperature and velocity of the particles as a function of time along with the average wall temperature and total energy stored in the bed. As expected, the average temperature of the bed gradually increases due to continuous irradiation with fluidization. Hence, the gas velocity increases, subsequently, the average particle velocity also increases as time progresses. As can be seen in the **FIGURE 5**, the average wall temperature is a function of bed temperature. Since the top semi-transparent wall is cooled down by convection, the average temperature of the frustum wall is significantly lower than the cylinder wall temperature. For 7 minutes of irradiation, about 0.206 kWh energy is stored in the bed.

SUMMARY

A transient numerical model has been developed, by coupling the discrete element method, computational fluid dynamics and discrete ordinate radiation models, to predict the particulate flow and heat transfer features of a fluidized bed reactor for solar thermochemical applications. The performance of the 30 kW_{th} reactor prototype has been studied using the chemically inert Geldart D type particles. Using the developed model, the fundamental granular flow characteristics can be obtained to enhance the design of the reactor.

ACKNOWLEDGMENTS

This study has been supported by the Tenure Track Program, The Ministry of Education, Culture, Sports, Science and Technology of Japan

REFERENCES

1. A. Steinfeld, Solar Energy. **78**, 603–615 (2005).
2. T. Kodama, S. Bellan, N. Gokon, H.S. Cho, Solar Energy **156**,113-132 (2017).
3. T. Nakamura, Solar Energy **19**, 467–475 (1977).
4. T. Kodama, N. Gokon, Chemical Reviews. **107**, 4048-4077 (2007).
5. S. Bellan, K. Matsubara, H.S. Cho, N. Gokon, T. Kodama, Powder Technology **319**, 228-237(2017).
6. S. Bellan, N. Gokon, K. Matsubara, H.S. Cho, T. Kodama, Energy **160**, 245-256 (2018).
7. S. Bellan, N. Gokon, K. Matsubara, H.S. Cho, T. Kodama, International Journal of Hydrogen Energy **43**, 16443-16457 (2018).
8. A. B Morris, Z. Ma, S. Pannala, C.M. Hrenya, Solar Energy **130**, 101-115 (2016).
9. M. Sandlin , S.I. Abdel-Khalik, Solar Energy **169**, 1-10 (2018).

10. S. Bellan, K. Matsubara, H.S. Cho, N. Gokon, T. Kodama, International Journal of Heat and Mass Transfer **116**, 377-392 (2018).
11. N.G. Deen, M.V.S. Annaland, M.A.V.D. Hoef, J.A.M. Kuipers, Chem. Eng. Sci. **62**, 28–44 (2007).
12. Y. Tsuji, T. Kawaguchi, T. Tanaka, Powder Technology, **77**, 79–87 (1993).
13. S. Bellan, J. Gonzalez-Aguilar, M. Romero, M.M. Rahman, D. Yogi Goswami, E.K. Stefanakos, D. Couling, Applied Thermal Engineering **71**, 481-500 (2014).